

32

153
P. 11

HIGH-LATITUDE COMMUNICATIONS SATELLITE (HILACS)

NAVAL POSTGRADUATE SCHOOL

N91-18145

The Naval Postgraduate School in the AE 4871 Advanced Spacecraft Design course has designed a communications satellite (HILACS) that will provide a continuous UHF communications link between stations located north of the region covered by geosynchronous communications satellites. This area (above approximately 60° N) will be served via a relay net control station (NCS) located with access to both the HILACS and geosynchronous communications satellites. The communications payload will operate only for that portion of the orbit necessary to provide specified coverage. The satellite orbit is elliptic with perigee at 1204 km in the southern hemisphere and apogee at 14,930 km with 63.4° inclination. Analysis and design for each of the subsystems was done to the extent possible within the constraints of an 11-week quarter and the design and analysis tools available. Work was completed in orbital analysis, the reaction control subsystem (RCS), attitude control subsystem (ACS), electric power subsystem (EPS), telemetry, tracking, and control (TT&C), thermal control subsystem, and the structures subsystem. The design team consisted of 12 students. Additional support was provided by the Jet Propulsion Laboratory and the Naval Research Laboratory.

SPACECRAFT DESCRIPTION

The High-Latitude Communications Satellite (HILACS) will provide a continuous UHF communications link between stations located north of the region covered by geosynchronous communications satellites, i.e., the area above approximately 60° N latitude. HILACS will also provide a communications link to stations below 60° N via a relay net control station (NCS), which is located with access to both the HILACS and geosynchronous communications satellites. The communications payload will operate only for that portion of the orbit necessary to provide specified coverage.

The satellite orbit is elliptic with perigee at 1204 km in the southern hemisphere and apogee at 14,930 km. The orbit inclination is 63.4° to eliminate rotation of the line of apsides. The orbit period is 4.8 hr, during which each spacecraft will be operating approximately 1.6 hr. The complete constellation will consist of three spacecraft equally spaced in mean anomaly.

The reaction control subsystems (RCS) and the stationkeeping propulsion subsystem is a monopropellant hydrazine system. There are four 38-N thrusters for the initial apogee adjustment and twelve 2-N thrusters for the RCS and stationkeeping. The propellant is contained in four tanks with internal pressurant bladders.

The satellite is three-axis-stabilized by four reaction wheels with thrusters providing redundancy and reaction wheel desaturation. The spacecraft is nadir-pointing with antenna-pointing accuracy of $\pm 0.5^\circ$. The satellite rotates about its yaw axis so as to maintain the solar panel axis (roll axis) normal to the sun line, providing maximum solar power efficiency. The attitude control subsystem (ACS) will utilize four sun sensors, two Earth sensors, and a three-axis rate-sensing gyroscope. The orientation of the four reaction wheels provides redundant operation.

The electric power subsystem (EPS) is a single bus, fully regulated system with bus voltage of 28 V. The EPS consists of two solar array panels, a 16-cell, 12 amp-hour nickel-

hydrogen battery, power control circuitry, and a shunt resistor bank. The EPS provides 343 W at end-of-life (EOL) at aphelion with a 10% margin. The solar array is comprised of GaAs solar cells, selected for their superior radiation tolerance.

The telemetry, tracking, and control (TT&C) subsystem design provides for both autonomous operations and direct control by a midlatitude ground-control station. The NCS will also be able to perform some TT&C functions.

The thermal control subsystem is primarily a passive system, with radiators on the satellite faces mounting the solar array panels, which will always be oriented parallel with the sun line. The other surfaces of the spacecraft will be insulated to maintain internal temperatures within acceptable limits. The passive system is augmented by heaters for equipment/locations requiring unique treatment.

The primary spacecraft structural support is the central tube, which provides the load-bearing structure for the equipment panels and fuel tanks. The central tube is also designed to provide for the design loads resulting from stacking of three satellites for launch.

Launch and Orbit Sequence

Figure 1 shows the launch configuration. All three satellites will be launched simultaneously on a single Delta/STAR 48 launch vehicle. The launch will take place from the Kennedy Space Center, and will place the three satellites initially into a 15,729 km \times 1204 km orbit at the desired inclination (Fig. 2). The launch vehicle final stage will provide active control for stabilization for the three stacked spacecraft while in ascent, elliptical parking orbit, and prior to each spacecraft's separation. As each satellite is separated from the final stage it will be spinning about a stable axis, eliminating the need for additional stabilization during the sun/Earth acquisition phase. Again, attitude stability is provided by the final stage of the launch vehicle for the still attached spacecraft. In this initial

PAGE 152 INTENTIONALLY BLANK

PRECEDING PAGE BLANK NOT FILMED

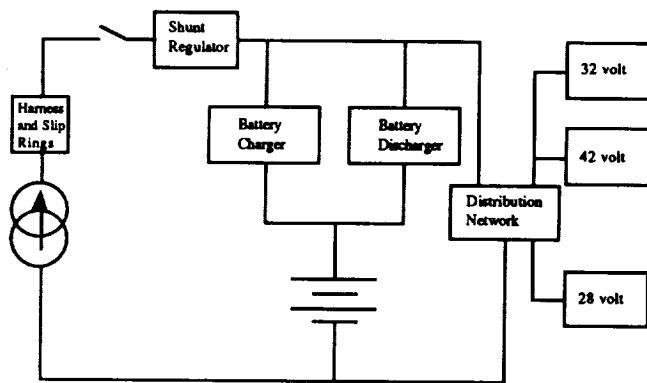


Fig. 1. Launch Configuration

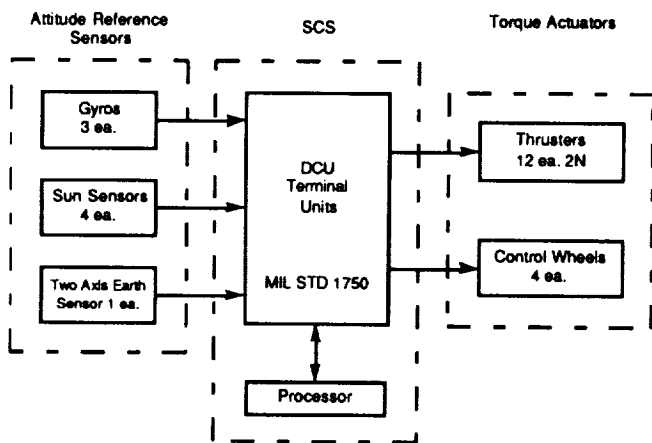


Fig. 2. Transfer Orbit Sequence

orbit, each spacecraft will acquire the sun and then the Earth to assume their Earth-pointing, three-axis stabilized configuration. The following sequence will then occur: solar arrays deploy, allowing electrical and thermal stability; the trailing satellite in the launch orbit will be reoriented and perform a perigee burn of 1.73 min using the four 38-N thrusters (-42.2 m/sec ΔV); orbit insertion of spacecraft into the 14,933 km \times 1204 km mission orbit. Since the mission orbit has a 4.8 hr period compared to the 5.0 hr period of the launch orbit, the second spacecraft will be aligned for insertion 8 orbits later, with the final spacecraft aligned following an additional 8 orbits. This sequence will put the entire plane of satellites in position 80 hr after the initial spacecraft is inserted into the mission orbit. This relatively long period between the insertion of each satellite also provides for the accurate determination of orbital parameters of the preceding spacecraft and adjustment on subsequent insertions as needed. The spacecraft on-orbit configuration is shown in Fig. 3.

Station Keeping/Orbit Perturbations

The time rate of change of inclination due to the gravitational effects of the Moon and the Sun were computed. In both cases, the rate is periodic in the right ascension of the orbit-

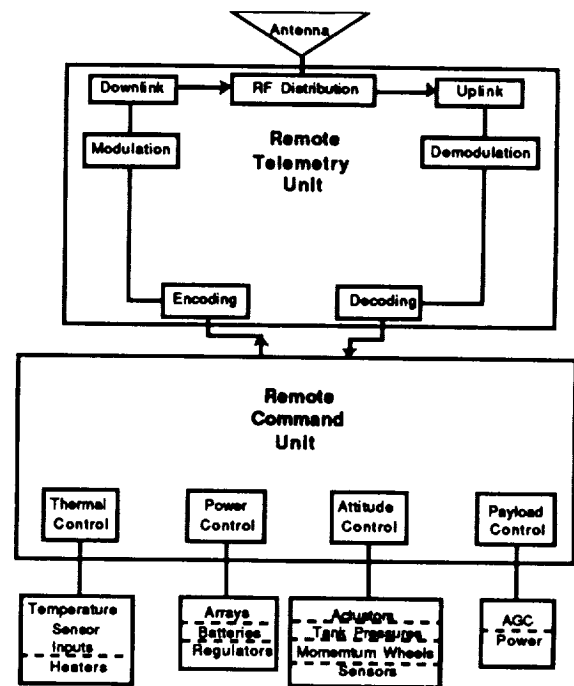


Fig. 3. On-Orbit Configuration

ascending node, which is decreasing at the daily rate of -0.425° . This causes the inclination rate to cycle completely in 847 days, with a maximum value of $0.1175^\circ/\text{yr}$ throughout the 3-year lifetime of the satellite. Since this represents the worst case alignment of the sun and the Moon during the mission, the actual values should be computed for these bodies based on their true positions for a given launch date recognizing that the resulting perturbation would actually be no larger than $0.1175^\circ/\text{yr}$. The error in inclination that would accumulate would only be that which represents the satellite life beyond one of the 847-day cycles. With this small change in inclination there is no need to budget propellant for station keeping due to inclination drift.

Argument of Perigee

Even though the satellites will be placed at the critical inclination, there will be drift of the argument of perigee due to higher-order effects. The long-period dynamic equations (normalizing the system to remove those short-period terms dependent only on mean anomaly) of the mission orbit were numerically integrated using a Runge-Kutta 4th-order fixed-step integrator. The analysis included perturbations to a Keplerian orbit due to the J₂, J₃, J₄, J₅ zonal harmonics. Although the mission orbit proves to be very stable in argument of perigee having drift through 360° with a period of 1100 yr, $0.33^\circ/\text{yr}$, the orbit is very sensitive to errors in inclination. A 0.1° error in inclination increases circulation of the argument to a rate of $1.44^\circ/\text{year}$. There is no need to budget propellant to correct for this small amount of drift for

the three-year lifetime. Propellant has been budgeted to correct drift of the argument of perigee through four years since the solar array has the capacity to provide power for more than the planned three-year satellite life. This station keeping will require a change in direction of the spacecraft velocity vector of 1.44° each year, representing a change in velocity of 133.7 m/sec. Using the attitude control thrusters, this will require a total of 81.8 kg (180 lbm) of propellant over 4 years. The current satellite design provides adequate capacity for this requirement as well as approximately 50 kg of additional propellant as margin.

The satellite is required to be Earth pointing and have solar array in direct view of the sun. The amount of yaw required each orbit is a function of the angle β between the solar orbit plane and the satellite orbit plane. This relationship is given in the following equation⁽¹⁾

$$\beta = A(B \sin \gamma \cos \Omega - \cos \gamma \sin \Omega) - C \sin \gamma$$

where β = orbit plane illumination angle; $A = \sin(i)$; i = orbit inclination = 63.435°; $B = \cos(\epsilon)$; ϵ = solar orbit inclination = 23.44°; $C = \cos(i) \sin(\epsilon)$; γ = sun central angle (measured ccw from vernal equinox to current position of sun relative to Earth); Ω = right ascension of the satellite orbit ascending node.

The angle between the solar array normal and the incident sunlight is given by the following equation⁽²⁾

$$\cos \theta = (\cos \alpha \cos \rho \sin \beta + \sin \alpha \cos \tau \cos \beta - \cos \alpha \sin \rho \sin \tau \cos \beta)$$

where $\cos \theta$ = angle between array normal and incident sunlight; α = array articulation angle between the array normal axis and the local horizontal, measured positive away from the Earth; ρ = spacecraft yaw angle measured ccw from inertial north; β = orbit plane illumination angle (see above); and τ = angle from solar noon, measured in the direction of the satellite orbit from the point on the orbit closest to the sun (local noon).

Solar Eclipse Periods

Batteries will be needed to provide power during solar eclipse. With a perigee of 1204 km, this will occur when orbit plane illumination angles are less than 57.3° ($\arcsin(\text{Re}/(\text{Re} + 650))$). Starting at zero for the orbit right ascension (Ω), and 180° for the sun central angle (γ), there will be 901 days out of the 1095 day planned lifetime during which the spacecraft will experience an eclipse of some duration. The resulting maximum solar eclipse period is 37.5 min during which the solar arrays are not illuminated. At 5 orbits per day, this specifies the need for batteries that can provide spacecraft bus power for up to 37.5 min through 4500 or more cycles.

SPACECRAFT CONFIGURATION

Equipment Layout

The primary considerations involved in developing the HILACS configuration were (a) to size the satellite for the Delta launch vehicle; (b) to shape the satellite and distribute masses to achieve the proper moment of inertia ratio for stability during a transfer orbit phase if required; (c) to use the east and west faces as equipment panels for thermal considerations since these faces will always be oriented parallel to the sun vector; and (d) to maintain as much modularity in the equipment layout as possible (see Figs. 4-7).

Four fuel tanks were used to achieve redundancy and to distribute the fuel mass. The basic shape of the satellite (1.9 m × 1.3 m × 0.7 m) was driven by the geometry of placing the four fuel tanks around the center tube within the Delta payload envelope. A fuel tank is mounted in each corner along the center line in height. The panels and component distribution are configured as shown in the figures for the spacecraft configuration.

Structures Subsystem

The spacecraft structural design is required to support the weight of three spacecraft under design loads for a Delta II (Table 1). The spacecraft employs identical designs for all three spacecraft, which forces an overdesigned structure for two of the three. Aluminum 6061-T6 was chosen for ease of machining and a favorable strength-to-weight ratio. The design supports loads through the central support assembly consisting of a frustum cone shell attached to the Delta II 3712B interface, a central cylindrical shell, and a similar frustum cone shell at the top of the spacecraft that attaches to the interface between each spacecraft.

Table 1. Design Constraints for Delta II Launch

Natural Frequencies	Lateral	Axial
Spacecraft	15 Hz	35 Hz
Equipment Panel	25 Hz	35 Hz
Solar Panel	35 Hz	-
Limit Loads		
Max. Lateral Condition	3.0 g	2.2 g
Max. Axial	-	6.0 g
Lateral Dynamic Loads	30 g	-
Factor of Safety = 1.5		
Margin of Safety = 10%		

A majority of the equipment mass is located on the east and west panels, which are designed to withstand 30 g and have a fundamental frequency above 25 Hz. The panels were designed to support 92.2 kg each of equipment mass. Load paths are provided to the central support assembly by means of panels attached to the north and south ends of the equipment panels. These support panels are also used to secure the four propellant tanks for axial loads. The panels are made of aluminum honeycomb material with core thickness 9.525 mm, and face thickness 0.912 mm. The same honeycomb

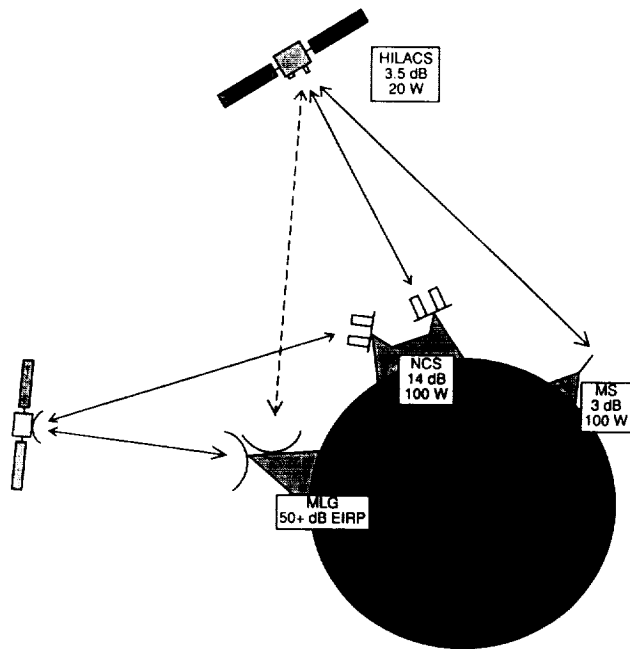


Fig. 4. East-Facing Panel

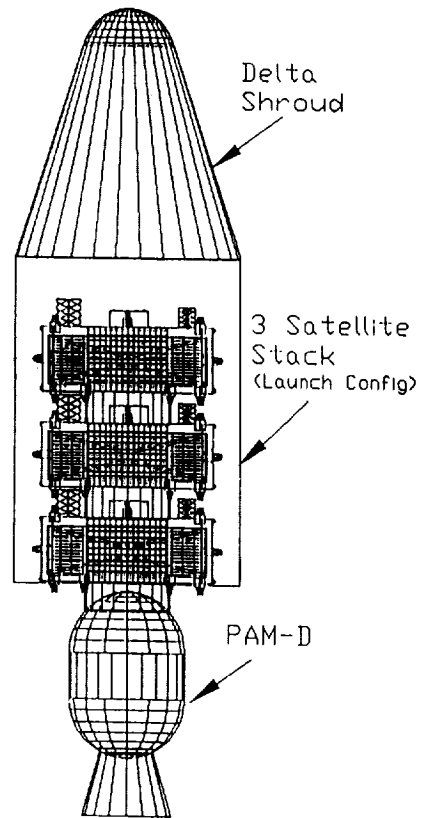


Fig. 5. View of Major Interior Elements

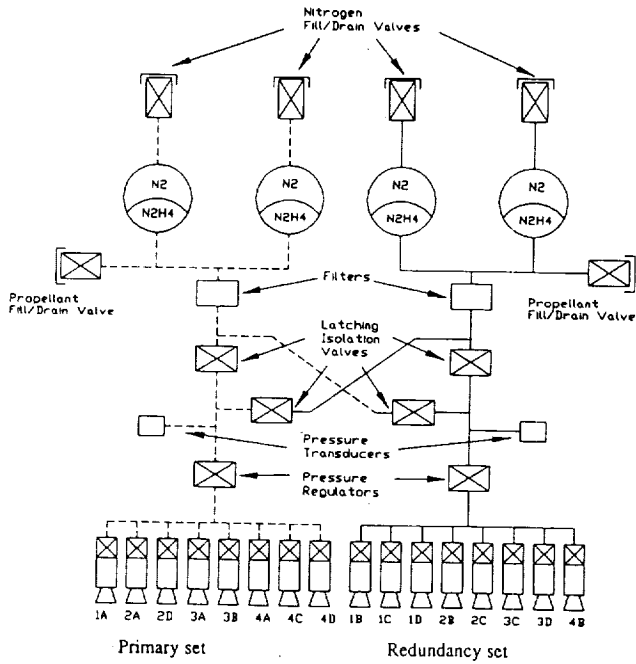


Fig. 6. Earth-Facing Panel

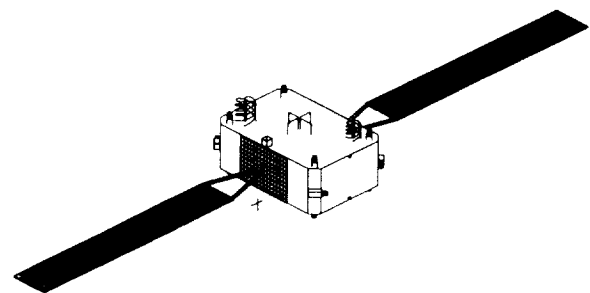


Fig. 7. West-Facing Panel

material is used for the equipment panels, propellant support panels, and spacecraft cover panels. Lateral load support for the propellant tanks is provided by struts attached to the top and bottom of the tanks and to the central support assembly.

The fundamental frequency estimated for the stacked configuration in lateral bending (6.22 Hz) was found to be well below the required 15 Hz for the Delta II launch. Because of this, the thickness values for the central support assembly were increased to raise the fundamental frequency for lateral bending. However, in the time of the course, the frequency issue was not resolved. The frequencies given from finite element analysis are shown in Table 2.

Table 2. Frequencies and Eigenvalues for Spacecraft

Mode	Frequency (cps)	Eigenvalue
1	42.71	7.2004D + 04
2	42.99	7.2946D + 04
3	68.02	1.8264D + 05
4	68.12	1.8318D + 05
5	80.69	2.5706D + 05
6	81.47	2.6201D + 05
7	103.99	4.2690D + 05
8	119.52	5.6391D + 05
9	129.11	6.5813D + 05
10	129.39	6.6095D + 05

Mass Summary (Tables 3-5)

Table 3. Mass Budget

Subsystem	Mass (kg)
TT&C	13.712
Payload	21.871
Attitude Control System	17.130
Electrical Power System	48.550
Reaction Control System	34.666
Thermal Control System	42.634
Structure	46.622
Dry Mass	225.185
Propellant	145.212
Wet Mass	370.397
Margin	41.520
Total Mass	411.917

Table 4. Propulsion Mass Breakdown

Item	Mass (kg)
Propellant (station keeping)	136.77
Propellant (ΔV change)	7.21
Propellant (desaturation)	1.00
Twelve 2-N Thrusters (12 \times 0.319 kg)	3.83
Four 38-N Thrusters (4 \times 0.735 kg)	2.94
Tanks (4 \times 5.897 kg)	23.59
Tubings, Valves, and Fittings	4.31
Nitrogen Pressurant	0.23
Total	179.88

Table 5. Structural Mass Summary

Structural Element	Mass (kg)
West Face Equipment Panel	0.918
East Face Equipment Panel	0.918
Lower Frustum of Cone	9.082
Cylindrical Support	8.192
Upper Frustum of Cone	5.221
(4) Propellant Support Panel	0.162
(8) Short Hollow Circular Strut	0.271
(8) Long Hollow Circular Strut	0.383
(4) Attachment Panel	0.086
North Face	0.624
South Face	0.624
Earth-Facing Panel	1.670
Anti-Earth-Facing Panel (with hole)	1.179
Structural Fasteners/Brackets	1.840
(2) Conical Support Ring	0.274
(2) Cylinder Support Ring	0.163
(4) Tank Ring	1.180
Support Structure Assembly Fittings	4.536
Total	46.622

Power Summary (Tables 6 and 7)

Table 6. Satellite Power Summary

Power Requirements	Power (W)
Payload	101.05
TT&C	11.22
EPS	20
ACS/RCS	70
Thermal Control	50
Wire Losses	7.05
Total Loads	259.32
Battery Charge Power	52.5
Total Sunlight Load	311.82
Ten Percent Margin	31.18
Total Design Power	343.00

Table 7. Eclipse Loads

Eclipse Power Requirements	Power (W)
EPS	20
ACS/RCS	70
Thermal	50
Total Eclipse Loads	140

PAYLOAD

System Description

The communications operations are shown in Fig. 8. The mission dictates a highly elliptic orbit at a 63.4° inclination. The ground stations are assumed to be located anywhere above 60° N latitude. To link these stations with a geosynchronous satellite, a central station acting as a hub must be located within the footprint of a geosynchronous satellite and HILACS. The location of this net control station (NCS), must be approximately 60° N latitude. A fourth site must be considered as well. This site is the source for data transmitted to the geosynchronous satellite and is assumed the ground control

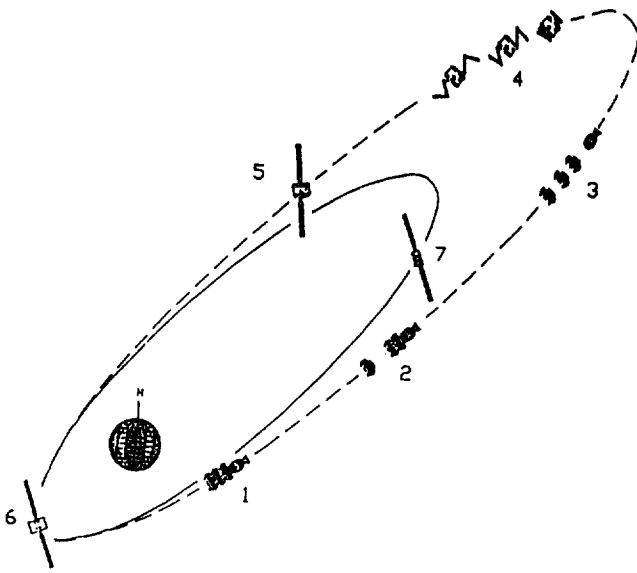


Fig. 8. Schematic of Communications Operations

site for its net of satellites including HILACS. It will be assumed that this station is located approximately 40° N (maximizing the number of locations on the Earth) and will be designated the midlatitude ground station (MLG).

The communication system operates at UHF with an uplink frequency of 350 MHz and a downlink frequency of 253 MHz. The link will operate at a data rate of 4800 bps using coherent BPSK modulation. A linear block error correction coding scheme is used resulting in a coded bit rate of 9600 bps.

The net operates in a hub-polling scheme in which the NCS controls access to the net in accordance with the needs of the users. This style of operation permits a variable number of users and maximizes the channel's data rate for this simplex link. The NCS polls each station prior to transmit to ensure it is ready to receive data and to find out whether they have any data to transmit. The NCS then relays data from the MLG (via a geosynchronous satellite) and from other stations on the net to the specific station. It then receives data from the station and readdresses these messages for further relay. It then repeats the process for each station on the link.

The NCS monitors satellite positions and ephemeris and predicts the position of the next ascending satellite. It establishes a link with the ascending satellite and performs a systems check prior to its activation. The NCS then determines the optimal altitude to introduce this satellite into the net and to release the descending satellite. It is conceivable that the NCS could operate two satellites simultaneously to ensure the most reliable communications throughout the region above 60° N latitude. The NCS also monitors the satellite health transmitted via the link.

The mobile ground stations, having a wide beamwidth and low-gain antennas, need only turn on their receivers to the default position and wait to be polled. Once polled, they establish link and move to an allocated slot for the remainder of their time on the link.

Design and Hardware

A bit-duration bandwidth product of 2.0, resulting in a bandwidth of 19.2 kHz is used as a compromise between minimizing the noise bandwidth and the intersymbol interference for this link. The MLG is assumed to be an established site with a high-gain helical antenna array with 25 dB of gain, transmitter with up to 1000 W (30 dBW) capability [so it will be optimally adjusted to maintain an EIRP ($P_t G_t$) just below saturation for the satellite system], and a receiver system with an effective temperature (T_e) of 150 K.

The NCS has two sets of helical arrays with 14 dB of gain. The station will require two of these antennas to provide a link with the active descending satellite and the ascending satellite in preparation for its activation. The effective noise temperature (T_e) at the receiver front end is computed to be 290 K for a noise figure of 3 dB relative to 290 K. It will be assumed that this station can transmit with a power of 100 W (20 dBW). The ground stations are assumed to be mobile, limiting their antenna to a crossed dipole design with a gain of 3 dB. The receivers' noise figure is 6 dB causing them to have T_e s of 865 K. The station's transmit power is also assumed to be 100 W (20 dBW). The satellite antennas have gains of 3.5 dB with a transmit power of 20 W (13 dBW). The receiver's noise figure is assumed to be 2 dB.

The system temperature is calculated after the antenna cable and at the receiver front end. The receiver noise figures relative to 290 K were listed earlier; the coaxial cable temperature is also assumed to be 290 K for each system. The antenna temperature (T_a) is dependent upon the gain of the antenna and the direction it is pointing. The MLG, with its relatively high-gain antenna, pointing away from the Earth has an assumed temperature of 150 K. Because the NCS and the mobile stations have low-gain antennas with a correspondingly wider field of view, their T_a is assumed to be approximately the temperature of the Earth, or 290 K. Since the satellite's antenna is pointing at the Earth, its T_a is also equal to 290 K.

The losses associated with the link equations are atmospheric loss, which is negligible for UHF, and free space loss, which is approximately 190 dB for the ranges in this link. Since this link is operated at a relatively low channel capacity, a relatively large bandwidth of twice the bit rate, or $2R_b$, is used minimizing the effect of intersymbol interference (ISI). Because the geometry will be changing due to the relative motion of the satellite and ground stations, the effect of fading will be time varying. Terrain effects can be minimized by optimizing the location of the ground station. To decrease the effect of the fading, which will appear in the form of a "burst error," a linear block code is used in the signal. This block code with a code rate of twice the data rate is effective when fades last for short periods of time. If long-term effects plague the ground station, modifications may be necessary such as elevating the ground plane to limit multipath, adding a second antenna to create spatial diversity, installing a directional, tracking antenna, or moving the ground station to a site less susceptible to the effects of multipath. Interference effects will be due to harmonics of military UHF voice communications.

These effects will be more transient than the fading effects, so the block coding should effectively minimize this interference effect.

For ideal stacking of the satellites on the launch vehicle, a maximum separation of 0.3 m was required. A resonant quadrifilar helix antenna was chosen since it is compact, has a wide beamwidth (approximately 110°), is simple in design, and has circular polarization. Analysis results in determining that quarter-turn, half-wavelength antennas with dimensions of approximately one-quarter wavelength for axial length and diameter are optimal for the dimensional constraints.

A crossed dipole antenna is used as a backup for the quadrifilar helixes and as the transmit and receive antenna for the TT&C system. It is composed of two orthogonal, center-fed, half-wavelength antennas⁽³⁾. The antenna is sized for the downlink frequency of 253 MHz, for a length of 0.593 m. It has a resonating circuit (a trap) that electrically shortens the antenna for the higher uplink frequency of 350 MHz or 0.429 m. The antenna is placed at 0.15 m above the ground plane to create the required radiation pattern⁽⁴⁾.

ELECTRICAL POWER SYSTEM DESIGN

The electrical power system (EPS) performs the functions of electrical power generation, storage, conditioning, and distribution for the on-orbit operation of the satellite. The majority of the generated power is consumed by the communications payload, with the balance used for the general operation of the spacecraft bus, attitude control, thermal control, TT&C, and the electrical power system itself. The communications payload system will operate only when the satellite ground track is above 50° N latitude. The TT&C system will operate only during sunlight periods of the cycle. The remaining systems will require power throughout the orbit.

The subsystem will be arranged as shown in Fig. 9. The shunt regulator will maintain the bus voltage at 28 V during sunlight periods and the battery charge/discharge unit is

responsible for maintaining eclipse loads and charging the battery. The arrays are switchable to allow for single array operation during periods when the required power is less than one array can supply. Auxiliary voltage levels of 32 and 42 V for use by the propulsion and attitude control subsystems will be generated from the 28-V bus using DC-DC converters.

EPS Design and Hardware Description

The solar arrays maintain normal incidence to the sun by having two degrees of freedom in the system: (1) satellite rotation about the yaw axis, and (2) solar array rotation about the array longitudinal axis. The arrays will be split into two independent, switchable systems with one array switched off-line until bus voltage demands. The cells used in the array have the following capabilities under AM0 conditions:

- $I_{sc} = 232.0 \text{ mA}$
- $V_{oc} = 1014.0 \text{ mV}$
- $I_{mp} = 219.5 \text{ mA}$
- $V_{mp} = 876.0 \text{ mV}$
- $P_{mp} = 192.3 \text{ mW}$
- Efficiency = 17.83%

Radiation effects on the solar cells are extreme due to passage through the lower portion of the Van Allen belts and represent the primary limiting factor of the satellite lifetime. Radiation received by the cells was calculated using tabulated data prorated for the fraction of time spent in orbit altitudes and summing the amounts received from the panel front and back over the three-year period. The array substrate thicknesses and shielding effectiveness are listed in Table 8⁽⁵⁾.

Table 8. Array Substrate Radiation Effects

Structure	Thickness (cm)	Shield Effectiveness (mm)
Thermal Paint	0.0043	0.03
Al Facesheet	0.013	0.16
Core Adhesive	0.007	0.06
Al Core	1.6	0.19
Core Adhesive	0.007	0.06
Al Facesheet	0.013	0.16
Epoxy/Glass	0.01	0.08
RTV-118	0.007	0.03
Total Thickness	1.6613	0.77
Back Shield Thickness (in ml)		30.315

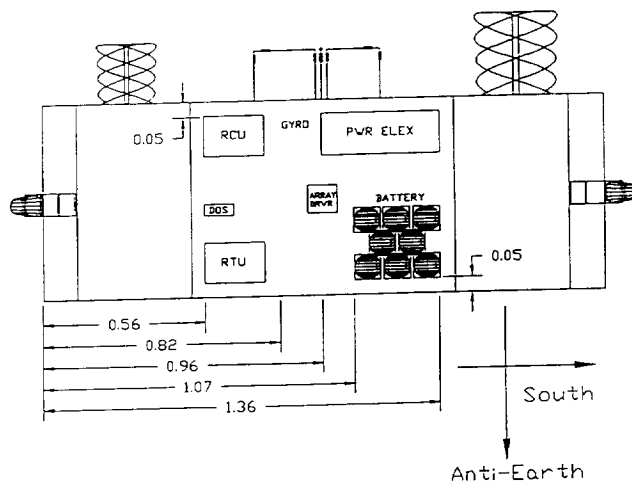


Fig. 9. Functional Block Diagram of EPS System

For an expected on-orbit life of three years, the total radiation received in one-MeV-equivalent electrons for front and back exposure is 5.14E + 15 for voltage and power and 2.82E + 15 for current. This equivalent radiation exposure results in degradation percentages for 12 ml liquid phase epitaxy (LPE) GaAs solar cells listed in Table 9. The radiation degradation experienced by 6-ml cells will be lower-resulting in higher EOL performance.

Table 9. Radiation Degradation Results

Cell Parameter	Final Parameter Percentages
V_{oc}	0.892
V_{mp}	0.86
I_{sc}	0.77
I_{mp}	0.768

An advantage of the GaAs cells over silicon cells is their stability at higher temperature. This stability becomes important as the array temperatures increase toward the end-of-life with decreasing array efficiencies. The design was iterated until the required EOL output power was achieved at an operating temperature consistent with the design array area. Worst case solar flux at aphelion with an array pointing error of 8.5° (0.15 rad) was assumed. The final design results are given in Table 10.

The power values for the satellite if launched at perihelion vice aphelion are a BOL power of 540 W and an EOL power of 382 W.

Table 10. Final Array Design

Cells in Series	44
Cells in Parallel	80
Total Number of Cells	3520
Total Array Area with Intercell Spacing	30,307.2 cm ²
Panel Dimensions (2.5 cm boundary on all sides)	0.487 m \times 3.305 m \times 1.74 cm
Array Mass	12.19 kg
Worst Case Operating Temperature	46.68°C
Minimum Eclipse Temperature	-117.88°C
Max. Power Output at 30.9 V	504 W
Minimum Power at EOL	357.53 W

Battery Design

The battery for eclipse power is a 12 amp-hour nickel-hydrogen battery manufactured by Eagle Picher. This battery is provided in a two-cell common pressure vessel (CPV) configuration. The battery voltage per CPV cell varies from 2.2 V to 3.2 V at full charge. For the bus configuration of a buck converter for constant current charge and a boost converter to maintain the line voltage, the number of CPV cells is limited to 8 for the 28-V bus. This gives a maximum battery voltage of 25.6 V and a minimum of 17.6 V.

The battery requirements are obtained from the eclipse load requirement of 140 W. With the boost converter efficiency of 85%, the actual power supplied by the battery during the eclipse period will be 164 W. The maximum eclipse period is 37 min of the 4-hr-48-min orbit. This gives a minimum recharge time of 4 hr 11 min. For the three-year projected mission lifetime, the satellite will experience a maximum of 4500 eclipse periods. Nickel-hydrogen batteries provide the highest capability of withstanding a large number of discharge cycles while still able to undergo large depths of discharge.

For a LEO satellite for which the charge and discharge cycles are numerous, the amount of energy that is removed from the battery must be replaced by an additional 10%. The charge rate chosen for this satellite is C/7. At this rate, the charging current is 1.7 A, and the maximum power required for charge,

including charger efficiencies, is 52.5 W. The time required for charging the battery after a discharge of 164 W at 17.6 V minimum for 37 min is determined by calculating the number of amp hours removed and adding 10%. For this design, 5.74 amp hours have been removed and will be replaced by 6.32 amp hours. Charging at 1.7 A yields a required charge time of 3.7 hr.

The power electronics control section of the power subsystem is responsible for maintaining the proper level of voltage for the satellite bus. The bus will be a fully regulated bus at 28 V. This regulation is accomplished by employing a shunt regulator for periods when the solar array is powering the spacecraft and by using a boost regulator for periods when the battery system is supplying the power. The bus voltage regulation accounts for a 1.3-V drop from the array slip ring and 0.8-V diode drops on each array and on each series string. A desired 30.9 V is then achieved at the array.

ATTITUDE CONTROL

The requirements for attitude dynamics and control (ADCS) are that the satellite be nadir pointing and three-axis stabilized. The communications system requires $\pm 2^\circ$ pointing accuracy. The ADCS system configuration (Fig. 10) is designed for a pointing accuracy of $\pm 0.5^\circ$. A monopropellant propulsion system is used that affects despin and desaturation, and sun-sensing capability to maximize solar array efficiency. The system is designed to be single-fault tolerant.

The ADCS performs in two modes, transfer orbit and on-orbit. The satellite will be ejected from the Delta launch vehicle with between 30 and 100 rpm during transfer orbit. The system will then despin the satellite after ejection, acquire the sun with sun sensors, despin completely, and acquire the Earth. After despin, the solar cells will deploy, and the reaction wheels and gyros will activate. The ADCS will maintain three-axis stabilization during transfer orbit burn to maintain solar power. Once on orbit, the ADCS will reacquire the Earth with the Earth sensor, and the satellite will be oriented for full operation.

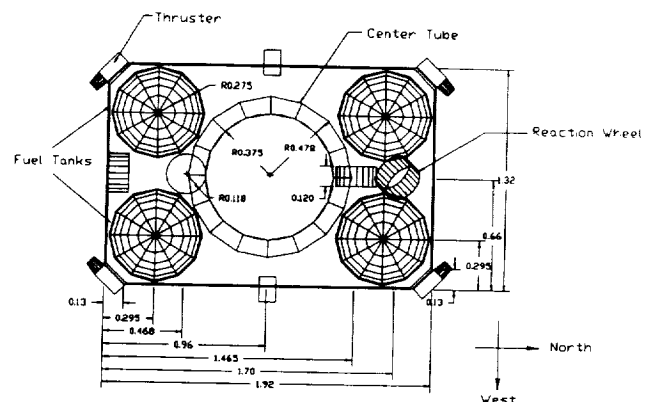


Fig. 10. ADCS Block Diagram

A four-reaction-wheel control actuator was chosen with three wheels along the roll, pitch, and yaw axis (initial spacecraft coordinates) and one wheel at a 45° angle for redundancy. The spacecraft will have additional redundancy for the control actuators provided by the thruster. The 2-N thrusters will be fired to desaturate the reaction wheels, despun the satellite and provide redundancy. The ADCS senses disturbance torques, due either to internally generated, solar pressure, or magnetic/gravitational torques, and provides the necessary attitude corrections. Internal torques are the dominant forces in wheel saturation. The internally generated torques arise from internal friction and instabilities. Thrusters will be able to desaturate the wheels quickly, with minimum pointing error.

The sensors for HILACS consist of an Earth (horizon) sensor, sun sensors, and rate gyros. The Earth sensor is a two-axis scanning conical-horizon sensor located near the antenna on the Earth face. Accuracy for a worst case pitch and roll error of $\pm 0.07^\circ$ at 1204 km can be achieved. Four two-axis sun sensors are mounted two each on the Earth and anti-Earth faces. The sun sensors provide yaw sensing with worst case error of $\pm 0.01^\circ$. One sun sensor will be able to give an accurate sun angle independent of the other sensor. This allows for nearly 4π steradians of coverage for the satellite. The redundant element is a three-gyro inertial-reference unit mounted inside the spacecraft. The outputs from the sensors are fed into the control computer for onboard processing. Commands are then sent to the actuators.

Components chosen for the ADCS are space qualified parts with pedigree characterized by previous flight performance. The sun sensors used are the coarse sun sensors flown on the INTELSAT VII satellite. The Earth sensors are manufactured by Barnes and well hardened for radiation tolerance. The rate measuring assembly was flown on INTELSAT V. The reaction wheels are made by Honeywell and were flown on DSCS III. The computer is a Mil Standard 1750 that is capable of providing autonomous control of the spacecraft.

TT&C

The highly elliptic orbit with inclination of 63.4° prevents continuous control of the satellite from the MLG station. The TT&C must, therefore, be capable of controlling the satellite operations for a significant part of its life (see Fig.11). When the satellite is in line of sight with the MLG it must be able to downlink its telemetry as well as respond to commands. These commands include initial maneuvers into operating orbit, modifications to current functions, and modifications to onboard programs to adapt the satellite to changes in operating conditions. Since the satellite cannot be continuously controlled by ground for many of its orbits, it will have the ability to link to the NCS during its operating cycle. During the time that it is linked to the NCS it will be polled as any other mobile station (MS). Once polled, it will downlink telemetry data specific to its operations such as transponder status and power system information.

The RTU interfaces with the telemetry antenna and the remote command unit (RCU). It performs all the functions of

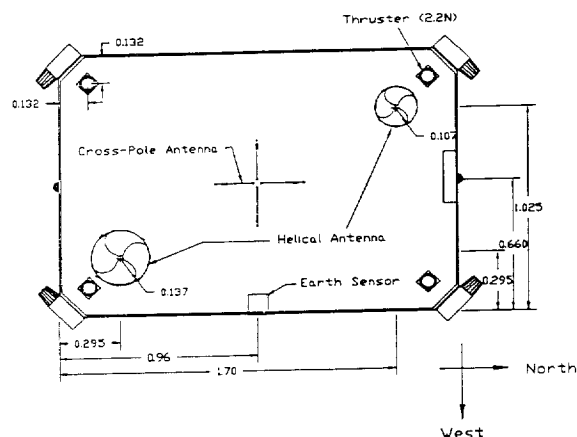


Fig. 11. TT&C Block Diagram

a transceiver including RF distribution to the single antenna, modulation, demodulation, and encoding/decoding of the telemetry data. The RTU uplink is at 350 MHz and its downlink is 253 MHz. The information is transmitted at a 1200-bps data rate, resulting in a 2400-bps transmission rate after encoding.

The RCU performs satellite control operations through the use of coded algorithms resident in memory. Dual microprocessors perform redundant operations based on these algorithms and their commands are correlated to remove the possibility of destabilizing operations due to single-event upsets (SEU). The RCU formats and relays telemetry to the RTU and acts on this telemetry in performing autonomous control of the satellite. The RCU also receives command signals from the RTU and performs these operations, which have priority over onboard generated commands.

The RTU uses a crossed-dipole hybrid antenna resonant at 350 MHz and 253 MHz. The RTU receives formatted commands from the RCU that are then encoded to modulation to the downlink frequency and transmitted. The RTU also demodulates and decodes uplinked telemetry commands to the acceptable format for the RCU. The RTU sends limited telemetry data to the NCS while performing transponder operations.

The RCU receives analog information from various sensors. It samples and performs pulse code modulation on the signals and then relays this data to the microprocessors for control functions.

The RCU commands heater operation based on temperature sensor data, and monitors voltages and currents to control the array drives, battery charging, solar array switching, and current regulation via the shunt regulator. The RCU also monitors the attitude control system and propulsion system operations by receiving data from the momentum wheels, Earth/sun sensors, thruster actuators, and propellant tank pressure sensors. The automatic gain control for the receiver and the transmit power of the transponder are monitored by the RCU.

PROPULSION SUBSYSTEM

The propulsion subsystem is a catalytic monopropellant hydrazine subsystem. The subsystem consists of four propellant

tanks with positive expulsion elastomeric diaphragms separating the pressurant from the propellant as shown in Fig. 12. The tanks are manifolded to two redundant sets of thrusters. The two sets of thrusters are interconnected and isolated by latching valves to provide redundancy for all on-orbit control functions.

After Delta II separation, the first of the three satellites will be slowed down to achieve the final orbit. Four 38-N thrusters and four 2-N thrusters will be fired at perigee to slow down the first satellite. The same procedure is repeated for each of the remaining two satellites for orbit insertion. Then only the 2-N thrusters will be used for roll, pitch, yaw desaturation, and despun.

The entire propulsion subsystem consists of four 38-N and twelve 2-N thrusters, four propellant/pressurant tanks made of titanium alloy, fill/drain valves for propellant and pressurant, latching isolation valves, filters, pressure regulators, pressure transducers, and lines made of titanium alloy.

The Delta II launch vehicle was chosen primarily because of its adaptability and cost. The Taurus and Atlas II launch vehicles will also satisfy the launch requirements.

The Delta II 7925 upper stage consists of the Morton Thiokol Star 48B solid rocket motor, a cylindrical payload attach fitting with clamp assembly and four separation springs, a spin table with bearing assembly, and motor separation system. The upper stage also contains a nutation control system (NCS).

The Delta II 3712B attach fitting is the interface between the upper-stage motor and the spacecraft. It supports the clamp assembly that attaches the spacecraft to the upper stage and allows the spacecraft to be released at separation. It mounts the four separation springs, two electrical disconnects, even sequencing system, upper stage telemetry, and the NCS.

THERMAL CONTROL

Passive thermal control techniques are used throughout the satellite. Two radiators made of optical solar reflector material, each $0.9 \times 0.7 \text{ m}^2$ are placed on the east and west faces of the

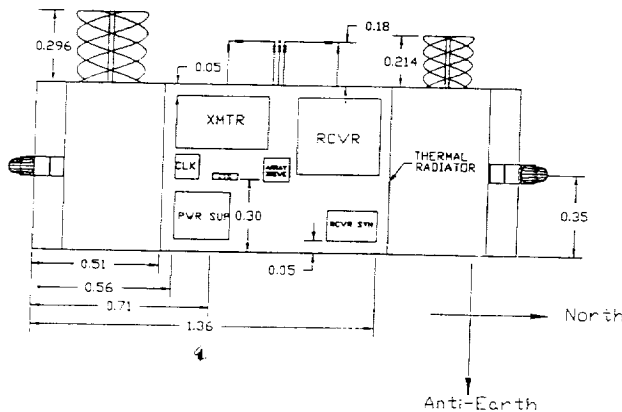


Fig. 12. Propulsion Subsystem

spacecraft. These faces are always edge on to the sun, thus receiving albedo and Earth radiated flux, but no solar flux.

All electronic modules are located on the equipment panels that are mounted back-to-back with the OSR to minimize conductive paths. The equipment panel is of aluminum honeycomb construction with aluminum heat sinks as required. No detailed thermal analysis of the substrates was attempted.

Multilayer Insulation (MLI)

MLI is used throughout to thermally isolate components. "Low" temperature applications use MLI with outside layers of aluminum kapton (spacecraft sides, etc.). "Hot" temperature locations use MLI with outside layers of titanium kapton (thrusters). A nominal thickness of 10 layers was used throughout. Temperature ranges for components are given in Table 11.

Table 11. Temperature Ranges for Components

Component	Operating Temp. (°C)
Electric power	
Control unit	-25/ + 30
Solar array	-160/ + 80
Shunt	-45/ + 60
Battery	0/ + 40
Payload	
Receiver electronics	-20/ + 45
Transmitter electronics	-15/ + 45
Antenna	-170/ + 90
Attitude control	
Earth/sun sensors	-25/ + 60
Angular rate assembly	-10/ + 60
Reaction wheels	-10/ + 55
Propulsion	
Tank	-5/ + 60
Valves	-5/ + 60
Thrusters	-5/ + 60

Two basic types of heaters are used: redundant and replacement. Redundant heaters are used as additional sources of thermal dissipation to maintain certain equipment (tanks, lines, valves, etc.) above minimum operating temperature. These consist of heat filament elements wound in layered material such as kapton. The other type of heater is the replacement heater, which is turned on when certain equipment (payload transmitter) is turned off in order to minimize thermal excursions. The former require additional power requirements whereas the latter do not. Thrusters have their own heaters for their catalytic beds. Heater control is either by enable/disable command from the ground, or once enabled, automatic control by thermistor to maintain temperatures within the allowed range.

Thermal design encompasses four phases of a satellite's life, namely prelaunch, launch, transfer orbit, and on-orbit. Only the on-orbit case was considered for this report. Analysis involved the two hot and cold steady-state cases. Internal sources include electronic equipment and soak-back from engine firings. External sources include solar, albedo, and Earth radiation. A thermal model was created identifying locations

of extreme temperatures for the satellite. Only a few iterations were done due to time constraints and availability of software tools.

ACKNOWLEDGMENTS

The project team would like to thank Prof. B. Agrawal for his guidance and support throughout this effort. We also want to thank Profs. R. Kolar, R. W. Adler, G. A. Myers, and A. Kraus, of the Naval Postgraduate School for their assistance. The following personnel from the Naval Research Laboratory also contributed to the success of the project: Mike Brown, Shannon Coffey, Chris Garner, Marv Levinson, and Tom Kawecki. Finally, we would like to thank Mr. J. D. Burke, our NASA center representative from the Jet Propulsion Laboratory (JPL), and Dr. J. H. Kwok also from JPL.

REFERENCES

1. NASA *Solar Cell Array Design Handbook*, Vol. I, equation 9.10-18, October, 1976.
2. NASA *Solar Cell Array Design Handbook*, Vol. I, equation 9.10-27, October, 1976.
3. John D. Kraus, *Antennas*, 2nd Ed., USA, McGraw-Hill, 1988.
4. Bruce S. Hale, *The ARRL Handbook for the Radio Amateur*, Sixty-sixth Ed., CT, American Radio Relay League, 1988.
5. JPL and NASA, *Solar Cell Array Design Handbook*, Volumes 1, p. 12.2-1. JPL Publication SP 43-38. October 1976.

